International Journal of Computational Methods
Vol. 7, No. 3 (2010) 421–442

DOI: 10.1142/S0219876210002283

World Scientific
www.worldscientific.com

ON A HIGH-RESOLUTION GODUNOV METHOD FOR A CFD-PBM COUPLED MODEL OF TWO-PHASE FLOW IN LIQUID-LIQUID EXTRACTION COLUMNS

D. ZEIDAN*

Department of Applied Sciences
Al-Balqa Applied University, Al-Salt, Jordan
dia@bau.edu.jo

M. ATTARAKIH

Chemical Engineering Department
Al-Balqa Applied University, Amman, Jordan

J. KUHNERT

Fraunhofer-Institut für Techno–und Wirtschaftmathematik
Kaiserslautern, Germany

S. TIWARI and V. SHARMA

Fachbereich Mathematik TU Kaiserslautern
Kaiserslautern, Germany

C. DRUMM and H.-J. BART

Lehrstuhl für Thermische Verfahrenstechnik
TU Kaiserslautern, Kaiserslautern, Germany

Received 25 February 2009
Revised 26 September 2009
Accepted 26 October 2009

This paper is about the numerical solutions for a computational fluid dynamics-population balance model (CFD-PBM) coupled model of two-phase flow in a liquid-liquid extraction column. The model accounts for a complete description between both the dispersed and continuous phases, and constitutes a hyperbolic system of equations having a linearly degenerate nature. A numerical algorithm based on operator splitting approach for the numerical solution of the model is used. The homogeneous part is solved using

*Principal and corresponding author.

the TVD MUSCL-Hancock scheme. Numerical results are presented, demonstrating the accuracy of the proposed methods and in particular, the accurate numerical description of the flow in the vicinity of the contact discontinuities.

Keywords: Two-phase flow; computational fluid dynamics (CFD); population balance model (PBM); hyperbolic balance laws; contact discontinuities; upwind Godunov methods.

1. Introduction

Accurate resolution of the dynamics related to liquid-liquid extraction columns is of high importance in a diverse range of industrial and engineering processes. The dynamic behavior of liquid-liquid two-phase flow in these columns is very complex and the basic principles governing the flow phenomena are not yet fully understood. In particular, the dispersed phase distribution has a strong effect in the hydrodynamic properties and phase distribution. However, a considerable effort has been made in order to develop polydisperse two-phase flow models with an inherent population balance model that will be able to consider the effects of the variations in the size and shape distributions of the dispersed phase. By introducing more fundamental models for the dispersed flow variables, a tool that can be employed for a variety of liquid-liquid extraction columns and conditions would be obtained. It is, therefore, a matter of interest for many industrial and technological applications to both model the mechanisms realistically and achieve accurate approximations to the solutions of initial and boundary value problems arising from the mechanisms and the model. On the other hand, the most advantageous model equations are that well developed theoretically and have various practical applications that are crucial to industry. Vast numbers of researches have been carried out for different applications in the context of problems arising in industrial applications in general and to liquid-liquid processes in particular (see, e.g. [Colella, *et al.* (1998); Gourdon *et al.* (1994); Hufnagl *et al.* (1991); Hultburt and Katz (1964); Kronberger *et al.* (1995); Ramakrishna (2000); Weinstein *et al.* (1998); Xiaojin *et al.* (2005)]).

The present article is directed towards an efficient and physically correct finite-volume computation of a particular combination of a liquid-liquid two-phase system within an extraction column. In this particular combination, we will refer to the primary liquid as the continuous phase while a dispersed phase to the secondary liquid that has been dispersed in the continuous phase. Once dispersed, the system will only remain so, at least in a terrestrial environment, if the primary phase is continually input into the system to maintain the dispersion. This is effectively done by ensuring that the dispersed phase always flows and then interactions are consequently transferred between phases in a continuously turbulent flow field. This results in fully phase distributions that provide a large number of interacting properties such as the evolution of the droplet distributions within the liquid-liquid process. The dynamics of these distributions can be captured with population balance equation models that describe the evolution of an appropriate distribution function with respect to various internal properties at a specific location in space. In general, the

population balance equation is coupled to integro-differential form of the governing equations that represent the driving force for particle growth [Ramkrishna (2000)]. The ability to solve population balance equations depends on the availability of valid mathematical models and robust numerical techniques. This is a very challenging task, as their analytical solutions are rare and the associated numerical methods must combine robustness and accuracy and cover a wide domain of physical conditions. This stresses the need to develop new population balance equation models and to have a variety of numerical schemes to investigate their properties by means of mathematical analysis. There are several different approaches that are commonly made to solve the population balance equations numerically. In most of these methods, an accurate simulation of the distribution is a challenging task as the changes in the distribution can be very sharp. Detailed reviews of previous work on solving population balance equations have been proposed in the literature and reviewed by many authors (see, e.g., [Kostoglou and Karabelas (1994); Lee (2001); Vanni (2000)] for a comprehensive review and references therein). Some typical ones are moment methods [Hultburt and Katz (1964)], characteristics method [Rhee *et al.* (2001)], weighted residuals [Singh and Ramkrishna (1977)], and Monte Carlo Method [Maisels *et al.* (1999)]. See [Gelbard *et al.* (1980); Hounslow *et al.* (1988); Marchal *et al.* (1988); Muhr (1996)] for a good and concise review of the up-to-date finite difference method. Recently, finite volume methods are implemented in the ParticleSolver software package for solving the population balance equations [Ma *et al.* (2002); Gunawan *et al.* (2004)].

In recent years, research has increased concerning the development of computational fluid dynamics (CFD) combined with the solution of population balance equations (see, e.g. [Vikhansky and Kraft (2004); Zucca *et al.* (2006)]). In the population balance model (PBM) together with CFD (usually abbreviated CFD-PBM coupled model) in the present work, the primary and secondary particle methods are utilized to reduce the bivariate population balance equations to a reduced dynamic model [Attarakih *et al.* (2006, 2008)]. In this paper, we propose a complete CFD-PBM coupled model by taking into account the momentum equation for the dispersed phase (see, e.g. [Tiwari and Kuhnert (2007)]) to the reduced PBM presented by Attarakih *et al.* [2006, 2008]. This result in a unified description of liquid-liquid two-phase flows, a well-defined mathematical structure and a successful numerical method and simulation tool for liquid-liquid extraction columns. Furthermore, this result in a fully hyperbolic conservative system of governing equations with source terms that provide a well-posed initial-value problem. Crucial new aspects of this CFD-PBM coupled model of liquid-liquid two-phase flow are the existence of real eigenvalues and a corresponding set of linearly independent eigenvectors. As a consequence, the model allows the application of advanced numerical methods as have been developed and successfully applied for problems in CFD. In addition, the model is well suited for using numerical methods specifically developed for one–phase fluid dynamics [Toro (1999)]. Thus, rather than developing new numerical algorithms specific to a CFD–PBM coupled model, we propose to adapt a general

purpose method for hyperbolic systems of conservation laws that can be applied to the model. We propose to use numerical methods based on operator-splitting approach [Yanenko (1971); Strang (1968)]. The splitting procedure separate the model equations into two problems: a homogeneous problem in which no sources are included and a second problem with the source terms only. This strategy enables the use of separate solvers for both the homogeneous problem in which discontinuities are present and for the non-homogeneous problem in which phase interaction occurs through the source terms. To solve the homogeneous problem in a robust way, we use Godunov methods of upwind type such as the first-order Godunov scheme [Godunov (1959)] and the second-order MUSCL-Hancock scheme [van Leer (1979)]. This solution is then utilized in the construction of splitting procedure to solve the general initial boundary value problem for the CFD-PBM coupled model.

The outline of the paper as follows. In the next section, we describe the CFD-PBM coupled model governing equations for liquid-liquid extraction columns. Hyperbolicity analysis of the model is developed in Sec. 3. A thorough description of the numerical treatment of the model equations is given in Sec. 4. This is followed in Sec. 5 with a detailed numerical results obtained by the proposed numerical methods. The important conclusions of this paper are summarized in Sec. 6.

2. CFD-PBM Coupled Model

The general liquid-liquid two-phase flow equations governing the CFD-PBM coupled model are presented hereafter. A system of differential equations is written without being established. The derivation of the balance equations is based on the concept of bivariate population balance equation and is well documented in the literature [Attarakih *et al.* (2006, 2008)]. In addition to the balance equations developed by Attarakih *et al.* [2006, 2008], an evolution equation for the dispersed-phase velocity is included and has incorporated exchange mechanisms that better describe dynamic compaction of liquid-liquid flows [Tiwari and Kuhnert (2007)].

In Eulerian frame of reference, the governing equations in the case of a one-dimensional (1D) incompressible liquid-liquid two-phase flow, in terms of conservative variables, reads as

$$\frac{\partial (N)_i}{\partial t} + \frac{\partial}{\partial z}((N)_i\ u_y) = (S_1)_i, \tag{1}$$

$$\frac{\partial (\alpha_y u_y)}{\partial t} + \frac{\partial}{\partial z}(\alpha_y\ u_y^2) = S_2, \tag{2}$$

$$\frac{\partial (\alpha_y c_y)}{\partial t} + \frac{\partial}{\partial z}(\alpha_y c_y u_y) = S_3, \tag{3}$$

$$\frac{\partial(\alpha_x c_x)}{\partial t} + \frac{\partial}{\partial z}(-\alpha_x c_x u_x) = S_4, \tag{4}$$

$$\frac{\partial(\alpha_y)_i}{\partial t} + \frac{\partial}{\partial z}((\alpha_y)_i\, u_y) = S_5. \tag{5}$$

Here, α_j is the volume concentration of phase j, $j = y$ (dispersed) and $j = x$ (continuous); N is the total number concentration; c_j is the solute concentration of phase j; u_j is the velocity of phase j. The notations $(\alpha_y)_i$ and $(N)_i$ denote the volume concentration and the total number of concentrations for the ith number of class of droplets with

$$\alpha_y = \sum_{i=1}^{\bar{n}} (\alpha_y)_i \quad \text{and} \quad N = \sum_{i=1}^{\bar{n}} (N)_i, \tag{6}$$

where $\bar{n}$ being defined as the number of classes of droplets in the dispersed phase.

Equations (1)–(5) with no viscosity effect express the total number of concentrations, the momentum of the dispersed phase, the solute concentrations of the dispersed and continuous phases, and conservation laws of volume of the dispersed phase. The source term $(S_1)_i$ in Eq. (1) represents the droplet breakage and coalescence defined only for one class, $i = 1$ as [Attarakih *et al.* (2006)]:

$$(S_1)_i = \Gamma(\bar{d})(\vartheta(\bar{d}) - 1)(N)_i - \frac{\omega(\bar{d})}{2}(N)_i^2, \tag{7}$$

where $\bar{d}$ is the mean particle diameter given by [Attarakih *et al.* (2008)]:

$$\bar{d} = \begin{cases} \sqrt[3]{\dfrac{6}{\pi}\dfrac{(\alpha_y)_i}{(N)_i}}, & (N)_i > \sqrt{\epsilon}, \\ d_{vs}, & \text{otherwise.} \end{cases} \tag{8}$$

In Eq. (8) ϵ is the machine precision and d_{vs} is the Sauter mean droplet diameter estimated from the available correlations in extraction columns [Schmidt *et al.* (2006)]. In this work, d_{vs} is taken as

$$d_{vs} = \frac{d_{\min} + d_{\max}}{2}, \tag{9}$$

where $d_{\min}$ and $d_{\max}$ are constants to be specified. These stands for minimum and maximum droplet diameters for the inlet feed distribution.

The first term in Eq. (7) contains the rate of formation of particles with breakage frequency Γ together with the mean number daughter particle ϑ. The second term represents the net rate of droplet death due to the coalescence of two droplets of the same mean size and concentration with frequency ω.

The source term in Eq. (2) is [Tiwari and Kuhnert (2007)]:

$$S_2 = \frac{\alpha_y}{\rho_y}(\rho_x - \rho_y)g - \alpha_y \mathrm{F}_{\mathrm{drag}} - \frac{\alpha_y}{\rho_y}\frac{\partial P}{\partial z} \tag{10}$$

and describes the momentum exchange mechanisms; ρ_j is the density of phase j and g is the gravitational force that regarded as given constants. The pressure P is assumed the same for both phases and defined as

$$P = \rho_x g\, z. \tag{11}$$

The drag force $\mathrm{F}_{\mathrm{drag}}$ is given by

$$\mathrm{F}_{\mathrm{drag}} = \frac{3}{4}\frac{\rho_x}{\rho_y}|u_y + u_x|(u_y + u_x)\frac{\mathrm{C_D}}{\bar{d}}. \tag{12}$$

The drag coefficient C_{D} in Eq. (12) is given by [Schiller and Naumann (1933)]:

$$\mathrm{C_D} = \begin{cases} \dfrac{24}{\mathrm{Re}}\,(1 + 0.15\ \mathrm{Re}^{0.687}), & \mathrm{Re} \le 1000, \\ 0.44, & \mathrm{Re} > 1000, \end{cases} \tag{13}$$

where the relative Reynold number (Re) defined as

$$\mathrm{Re} = \bar{d}|u_y + u_x|\frac{\rho_x}{\mu_x} \tag{14}$$

and μ_x is the viscosity of the continuous phase, which is a constant to be specified.

The source terms S_3 and S_4 in Eqs. (3) and (4) are the mass transfer coefficients defined as [Attarakih *et al.* (2006)]:

$$S_3 = 6K_{_{0y}}(\mathfrak{m}\, c_x - c_y)\frac{\alpha_y}{\bar{d}} \quad \text{and} \quad S_4 = -S_3, \tag{15}$$

where K_{0y} is the overall mass transfer coefficient and $\mathfrak{m}$ is the solute distribution coefficient.

Finally, the source term S_5 in Eq. (5) is set to zero for only one class, $\bar{n} = 1$, throughout this work.

To close the system, the following additional relations are used

- The volume fractions are related by

$$\alpha_x + \alpha_y = 1. \tag{16}$$

- The continuous phase velocity u_x is defined as [Attarakih *et al.* (2006)]:

$$u_x = \frac{Q_x^{\mathrm{in}}}{A_c}\frac{\Delta_x(z)}{\alpha_x}, \tag{17}$$

  where A_c is the column cross-sectional area, Q_x^{in} (in stands for inlet) is the continuous phase volumetric flow rate which is regarded as a given constant and Δ_x is the step function given as

$$\Delta_x = \begin{cases} 1, & z \le z_x, \\ 0, & \text{otherwise}, \end{cases} \tag{18}$$

  for $z \in (z_y, z_x)$ with z_y and z_x are the inlets of the dispersed and continuous phases, respectively.

In the next section, we consider whether or not the model is hyperbolic for the liquid-liquid column under investigation.

3. Hyperbolicity Analysis of the CFD-PBM Coupled Model

In this section, a study of the characteristics (hyperbolicity) of the model equations is presented. It is necessary to check the hyperbolicity of the equations. This is useful in showing the range of validity of the model and in developing successful numerical methods.

3.1. *Formulations*

The CFD-PBM coupled model Eqs. (1)–(5) can be expressed in vector form as

$$\frac{\partial \mathbb{U}}{\partial t} + \frac{\partial \mathbb{F}(\mathbb{U})}{\partial z} = \mathbb{S}(\mathbb{U}), \quad z \in \mathbb{R}, \ t \in \mathbb{R}^+, \tag{19}$$

with

$$\mathbb{U} = \begin{pmatrix} (N)_i \\ (\alpha_y)_i \\ \alpha_y u_y \\ \alpha_y c_y \\ \alpha_x c_x \end{pmatrix}, \quad \mathbb{F}(\mathbb{U}) = \begin{pmatrix} (N)_i \ u_y \\ (\alpha_y)_i \ u_y \\ \alpha_y u_y^2 \\ \alpha_y c_y u_y \\ -\alpha_x c_x u_x \end{pmatrix}, \tag{20}$$

$$\mathbb{S}(\mathbb{U}) = \begin{pmatrix} \Gamma(\bar{d}) \ (\vartheta(\bar{d}) - 1) \ (N)_i - \frac{\omega(\bar{d})}{2} \ (N)_i^2 \\ S_5 \\ \frac{\alpha_x}{\rho_y}(\rho_x - \rho_y)g - \alpha_y \ \mathrm{F}_{\mathrm{drag}} - \frac{\alpha_x}{\rho_y} \ \frac{\partial P}{\partial z}, \\ 6K_{0_y}(\mathfrak{m} \ c_x - c_y)\frac{\alpha_x}{d} \\ 6K_{0_y}(c_y - \mathfrak{m} \ c_x)\frac{\alpha_x}{d} \end{pmatrix}. \tag{21}$$

In Eq. (19) $\mathbb{U} \in \mathbb{R}^q$ represents the vector of conservative variables, $\mathbb{S} \in \mathbb{R}^q$ is the source term vector and $\mathbb{F} : \mathbb{R}^q \to \mathbb{R}^q$ is the flux vector ($\mathbb{R}$ is the set of real numbers and for $q \geq 1$).

To determine the classification of the model equations and to provide the mathematical framework needed for the development of the numerical methods, we give a standard formulation and analysis applicable to systems of first-order quasi-linear partial differential equations (PDEs). The analysis requires that Eq. (19) to be expressed in the following quasi-linear form

$$\frac{\partial \mathbb{U}}{\partial t} + \mathbb{A}(\mathbb{U})\frac{\partial \mathbb{U}}{\partial z} = \mathbb{S}(\mathbb{U}), \tag{22}$$

which is obtained by carrying out the differentiation of $\mathbb{F}$ with respect to z. The matrix $\mathbb{A}(\mathbb{U})$ is the Jacobian matrix defined by

$$\mathbb{A}(\mathbb{U}) = \frac{\partial \mathbb{F}}{\partial \mathbb{U}}. \tag{23}$$

Now, if we denote the components of $\mathbb{U}$ and $\mathbb{F}$ by u_j and f_j $(j = 1, \ldots 5)$, respectively, then $\mathbb{A}(\mathbb{U})$ is given by

$$\begin{pmatrix} \frac{\partial f_1}{\partial u_1} & \frac{\partial f_1}{\partial u_2} & \cdots & \frac{\partial f_1}{\partial u_5} \\ \frac{\partial f_2}{\partial u_1} & \frac{\partial f_2}{\partial u_2} & \cdots & \frac{\partial f_2}{\partial u_5} \\ \vdots & \vdots & \vdots & \vdots \\ \frac{\partial f_5}{\partial u_1} & \frac{\partial f_5}{\partial u_2} & \cdots & \frac{\partial f_5}{\partial u_5} \end{pmatrix}. \tag{24}$$

By direct evaluation of all partial derivatives, the following expression is obtained for $\mathbb{A}(\mathbb{U})$

$$\begin{pmatrix} u_y & -\frac{u_y (N)_i}{(\alpha_y)_i} & \frac{(N)_i}{(\alpha_y)_i} & 0 & 0 \\ 0 & 0 & 1 & 0 & 0 \\ 0 & -u_y^2 & 2u_y & 0 & 0 \\ c_y & -c_y u_y & c_y & u_y & 0 \\ 0 & 0 & 0 & 0 & -u_x \end{pmatrix}. \tag{25}$$

The matrix contains the velocity for both the dispersed and the continuous phases, the volume concentration, the total number of concentration for the ith number of class of droplets, and the solute concentration of the dispersed phase.

The mathematical analysis of Eqs. (1)–(5) can be formulated using variables other than the conserved variables. Alternative choice of formulation then is the vector of primitive or physical variables [Laney (1998)]. Mathematically, the vector of conservative variables $\mathbb{U}$ is more natural for expression as well as programming the governing equations than the primitive variables. From a numerical viewpoint, primitive variables are more convenient if we want to enforce the initial and boundary conditions and to display the numerical results. The primitive variables for a 1D CFD-PBM coupled model would be

$$\mathbb{W} = [(N)_i, (\alpha_y)_i, u_y, c_y, c_x]^T, \tag{26}$$

for which the governing equations take the form

$$\mathbb{B}(\mathbb{W})\frac{\partial \mathbb{W}}{\partial t} + \mathbb{A}(\mathbb{W})\frac{\partial \mathbb{W}}{\partial z} = \mathbb{Q}(\mathbb{W}), \tag{27}$$

where $\mathbb{Q}(\mathbb{W}) = (\partial\mathbb{W}/\partial\mathbb{U})\mathbb{S}(\mathbb{U})$ and the coefficient matrices are arranged as follows

$$\mathbb{B}(\mathbb{W}) = \begin{pmatrix} 1 & 0 & 0 & 0 & 0 \\ 0 & 1 & 0 & 0 & 0 \\ 0 & u_y & (\alpha_y)_i & 0 & 0 \\ 0 & c_y & 0 & (\alpha_y)_i & 0 \\ 0 & 0 & 0 & 0 & \alpha_x \end{pmatrix}, \tag{28}$$

$$\mathbb{A}(\mathbb{W}) = \begin{pmatrix} u_y & 0 & (N)_i & 0 & 0 \\ 0 & u_y & (\alpha_y)_i & 0 & 0 \\ 0 & u_y^2 & 2(\alpha_y)_i & 0 & 0 \\ 0 & u_y c_y & (\alpha_y)_i c_y & (\alpha_y)_i u_y & 0 \\ 0 & 0 & 0 & 0 & -\alpha_x u_x \end{pmatrix}. \tag{29}$$

3.2. *Mathematical property of the model equations*

The 1D Eq. (19) represents an initial-value problem (IVP) with initial conditions $\mathbb{U}(z,0) = \bar{\mathbb{U}}(z)$ in the range of $a \le z_j \le b$ for which $1 \le j \le q$ and $t \ge 0$. This IVP is well posed if system (19) has a unique solution on the differentiable interval value $\bar{\mathbb{U}}(z)$. In other words, if the coefficient matrix of the system has real eigenvalues, then the IVP is said to be a well-posed problem. If all the corresponding eigenvalues are linearly independent, then the system (1)–(5) is hyperbolic. More precisely, it is well known that the eigenvalues do not depend on the source terms and they represent the wave propagating speeds characterized by fluid properties and their dynamic interactions. For the characteristics analysis, therefore, one would works with the homogeneous form of both formulations, conservative (19) and primitive (27). Thus, we set $\mathbb{S}(\mathbb{U}) \equiv 0$ or $\mathbb{Q}(\mathbb{W}) \equiv 0$ to investigate the mathematical properties of the of the eigenvalues and eigenvectors. For both formulations, conservative and primitive, the eigenvalues associated with the CFD-PBM coupled model are determined by

$$\det[\mathbb{A} - \lambda I] = 0. \tag{30}$$

As a result, we derive a fifth-order polynomial equation as

$$P_5(\lambda) = (-u_x - \lambda)(u_y - \lambda)^4 = 0, \tag{31}$$

which gives the following real eigenvalues

$$\lambda_y = \lambda_{y_1} = \lambda_{y_2} = \lambda_{y_3} = \lambda_{y_4} = u_y, \quad \lambda_x = -u_x. \tag{32}$$

Clearly, the first eigenvalue, a multiple eigenvalue, represents the dispersed phase velocity while the second eigenvalue related to the continuous phase along the liquid-liquid extraction column. The two physic velocities appear here might not be in agreement with all current proposals on this subject and have no analogy in one-phase fluid dynamics. However, our present theoretical knowledge in this area is still insufficiently mature that a definitive judgment is not yet possible.

The existence of only real eigenvalues is a necessary but in itself insufficiently condition for the existence of a well-posed hyperbolic system of PDEs. A further requirement is the existence of a complete set of independent eigenvectors. On the other hand, this is a prerequisite for the proper applications of a number of advanced numerical techniques that make explicit use of the hyperbolic nature of the governing field equations. The eigenvectors of $\mathbb{A}$, $K^{(j)}$ $(j = 1, \ldots, 5)$, are solutions of the eigenvalue problem

$$\mathbb{A}K^{(j)} = \lambda_{\bar{i}} K^{(j)} \quad \bar{i} = y, x. \tag{33}$$

Here, we chose to present the corresponding right eigenvectors for the conserved formulation (19). Thus, the eigenvectors are

$$K^{(y)} = \begin{pmatrix} 0 \\ 1 \\ u_y \\ 0 \\ 0 \end{pmatrix}, \quad K^{(x)} = \begin{pmatrix} \frac{(N)_i}{(\alpha_y)_i} \\ 1 \\ -u_x \\ 0 \\ 0 \end{pmatrix}, \tag{34}$$

where the notations $K^{(y)}$ and $K^{(x)}$ represent the eigenvectors for the dispersed and continuous phases, respectively.

We end this section with the nature of the characteristic fields associated with each pair $(\lambda_{\bar{i}}, K^{(j)})$. The characteristic field associated with the continuous phase $(\lambda_x = -u_x)$ is found to be linearly degenerate

$$\nabla\lambda_x(\mathbb{U}) \cdot K^{(x)}(\mathbb{U}) = 0 \quad \forall\, \mathbb{U}, \tag{35}$$

while for the dispersed phase $(\lambda_y = u_y)$ we have

$$\nabla\lambda_y(\mathbb{U}) \cdot K^{(y)}(\mathbb{U}) = 0 \quad \forall\, \mathbb{U}, \tag{36}$$

which is also linearly degenerate.

The established eigenstructure shows that the CFD-PBM coupled model is hyperbolic with eigenvectors being linearly degenerate. They correspond to contact discontinuities (slip lines) [Chadwick (1976); Sychev *et al.* (2008)]. In applications, it is fairly typical that the linearly degenerate eigenvectors correspond to a multiple eigenvalues. An important observation is that only contact discontinuities are present in the solution of the model equations. The consequence of these contact discontinuities is not clear yet and further mathematical modeling research must be done in this direction.

4. Numerical Methods of Solution

Having formulated the mathematical structure of the CFD-PBM coupled model equations in the previous section, we will investigate its numerical approximation next. Before we begin, however, we need to get some ideas of what lies ahead. The model Eqs. (1)–(5) are sufficiently difficult to solve numerically to determine the

main features of the solution. This is due to the source terms on the right-hand side of the equations and to the mathematical nature of the characteristic fields as being linearly degenerate. As such, they pose extensive difficulties, even for computational methods, and it is agreeable that a detailed description of these difficulties is always desirable. As mentioned in the previous section, linearly degenerate fields correspond to contact discontinuities. These contact discontinuities require a correct wave speed of propagation, sharp resolution of the transition zone, and absence of spurious oscillations around shocks specially in long-time evolution as in the case of liquid-liquid extraction columns.

The numerical approach used in this paper to solve the CFD-PBM coupled model is based on the basis of finite volume techniques. The finite volume formulation for solving Eq. (19) reads [Toro (1999)]

$$\mathbb{U}_i^{n+1} = \mathbb{U}_i^n - \frac{\Delta t}{\Delta x}[\mathbb{F}_{i+\frac{1}{2}} - \mathbb{F}_{i-\frac{1}{2}}] + \Delta t\, \mathbb{S}_i, \tag{37}$$

where $\mathbb{U}_i^n$ is an approximation to the spatial-integral

$$\mathbb{U}_i^n = \frac{1}{\Delta z}\int_{z_{i-\frac{1}{2}}}^{z_{i+\frac{1}{2}}} \mathbb{U}(z, t^n)dz, \tag{38}$$

within the cell $[z_{i-\frac{1}{2}}, z_{i+\frac{1}{2}}]$ of length Δz, at time level n. $\mathbb{F}_{i+\frac{1}{2}}$ is the numerical flux and $\mathbb{S}_i$ is the numerical source terms.

A common practice to solve the system Eq. (19) by using splitting strategy (also called fractional step) [Strang (1968)]. First, the following hyperbolic system of conservation laws is solved using finite volume methods

$$\frac{\partial \mathbb{U}}{\partial t} + \frac{\partial \mathbb{F}(\mathbb{U})}{\partial z} = 0, \tag{39}$$

with the initial conditions $\mathbb{U}(z, t^n) = \mathbb{U}^n$, and its solution is then used as an initial conditions of the following ordinary differential equation problem

$$\frac{d\mathbb{U}}{dt} = \mathbb{S}(\mathbb{U}), \tag{40}$$

which is often solved with any classical numerical tool, such as the Runge–Kutta scheme, an explicit or implicit Euler scheme or any available scheme to obtain the complete solution of the system equations (19). The splitting procedure enables the use of separate solvers for both the homogeneous problem (39) in which discontinuities are present and for the nonhomogeneous problem (40) in which phase interaction occurs through the source terms. At this time, only Godunov methods of upwind type are considered for the homogeneous problem. These methods are characterized as being of first order or by their higher accuracy in the smooth regions of the solution without presenting the spurious oscillations associated with the conventional second-order methods in the presence of discontinuities. Godunov upwind-based methods are of great interest in numerous applications and have distinct features, as they resolve stationary and isolated waves exactly. The numerical methods of interest in this paper for solving the homogeneous problem

are the MUSCL–Hancock and Godunov methods. The Godunov scheme is a first-order upwind-type method [Godunov (1959)]. The MUSCL–Hancock technique [Van Leer (1979)] is a second-order accurate upwind method, and meets the total variance diminishing (TVD) requirements when employed with slope-limiter functions. Godunov's upwind scheme utilize the solution of the local Riemann problem with data $\mathbb{U}_L = \mathbb{U}_i^n$, as left data, and $\mathbb{U}_R = \mathbb{U}_{i+1}^n$, as right data, to define numerically the intercell flux, $\mathbb{F}_{i+\frac{1}{2}}$. The Riemann problem for the CFD-PBM coupled model is the initial-value problem for Eq. (39) in the domain $-\infty < z < \infty, t > 0$ with the special initial conditions

$$\mathbb{U}(z,0) = \begin{cases} \mathbb{U}_i^n & \text{if } z < z_{i+\frac{1}{2}}, \\ \mathbb{U}_{i+1}^n & \text{if } z > z_{i+\frac{1}{2}}. \end{cases} \tag{41}$$

For the CFD-PBM coupled model, the Riemann problem consists a repeated wave for both the dispersed and continuous phases. Therefore, the only possible wave combinations involving discontinuities are contact waves. The first-order Godunov scheme uses the state $\mathbb{U}_{i+\frac{1}{2}}$ along the t-axis ($z = 0$) to estimate the Godunov intercell numerical flux and then evaluating the physical flux vector $\mathbb{F}(\mathbb{U})$ in Eq. (39) at $\mathbb{U}_{i+\frac{1}{2}}(0)$, namely

$$\mathbb{F}_{i+\frac{1}{2}}^{\text{God}} = \mathbb{F}(\mathbb{U}_{i+\frac{1}{2}}(0)). \tag{42}$$

This first-order scheme can be extended to second-order accuracy in space and time following the MUSCL–Hancock approach. The MUSCL–Hancock technique has three steps to construct the numerical flux $\mathbb{F}_{i+\frac{1}{2}}$ in Eq. (37). These steps are summarized as follows.

Step I. *Data reconstruction.* The cell average variable $\mathbb{U}_i^n$ is locally replaced by piecewise linear functions in each cell.

$$\mathbb{U}_i(z) = \mathbb{U}_i^n(z) + \frac{(z - z_i)}{\Delta z}\bar{\Delta}_i, \tag{43}$$

where $\bar{\Delta}_i$ is a limited slope to avoid spurious oscillation near large gradients of the numerical solution and obtained using TVD constraints among various limiters [Toro (1999)]. Boundary extrapolated value $\mathbb{U}_i(z)$ is then given by

$$\mathbb{U}_i^{L,R} = \mathbb{U}_i^n \pm \frac{1}{2}\bar{\Delta}_i. \tag{44}$$

Step II. *Evolution.* The boundary extrapolated values $\mathbb{U}_i^L$ and $\mathbb{U}_i^R$ are evolved by half–time $\frac{1}{2}\Delta t$ as

$$\bar{\mathbb{U}}_i^{L,R} = \mathbb{U}_i^{L,R} + \frac{1}{2}\frac{\Delta t}{\Delta z}[\mathbb{F}(\mathbb{U}_i^L) - \mathbb{F}(\mathbb{U}_i^R)]. \tag{45}$$

Step III. *The Riemann problem.* In order to advance the solution in time a Riemann problem is solved on each cell to obtain numerical flux contributions with the evolved data $\mathbb{U}_L = \bar{\mathbb{U}}_i^R$ and $\mathbb{U}_R = \bar{\mathbb{U}}_{i+1}^L$ as follows

$$\mathbb{F}_{i+\frac{1}{2}} = \mathbb{F}(\mathbb{U}_{i+\frac{1}{2}}(0)). \tag{46}$$

Here, $\mathbb{U}_{i+\frac{1}{2}}(0)$ represents the value of the similarity solution $\mathbb{U}_{i+\frac{1}{2}}(\frac{x}{t})$ at $\frac{x}{t} = 0$. The numerical flux $\mathbb{F}_{i+\frac{1}{2}}$ is then obtained exactly in the same way as in the Godunov first-order upwind-type scheme.

5. Numerical Results

In this section, we present numerical results for the CFD-PBM coupled model (1)–(5) and compare the accuracy of the proposed numerical methods presented in the previous section. These numerical results were obtained using the splitting procedure with no source terms in Eqs. (1), (3), and (4). Physically, this means that we look at the experiments at a time when the droplet breakage and coalescence and the mass transfer coefficients are negligible. The results illustrate typical wave pattern for a Rotating Disc Contactor (RDC) liquid-liquid extraction column.

A liquid-liquid extraction column of 0.15 m diameter and 2.55 m height is simulated. The simulations were one dimensional. A summary of the column technical specifications is given in Table 1 [Attarakih *et al.* (2008)]. The numerical solutions are found in the domain $\mathcal{Z} = [z_0, z_H] = [0, 2.55]$ (in meters), and the domain consists of two sections $[0, z_y]$ and $[z_x, z_H]$ for the dispersed and continuous phases, respectively. The column is discretized with $M = 100$ computing cells for a coarse mesh and $M = 1000$ for a fine mesh with a CFL (Courant–Friedrichs–Lewy) condition of 0.0002. Transmissive boundary conditions are applied at $z = z_0$ and $z = z_H$. The SUPERBEE limiter was used to control the spurious oscillations associated with second-order MUSCL–Hancock scheme solutions. The SUPERBEE limiter has been our choice since it has shown a unique success in many practical computations (see, e.g. [Fraccarollo and Toro (1995); Romenski and Toro (2004); Zeidan *et al.* (2007a, b)] and references therein). For a detailed description of the available limiters, refer to the work done by Toro [1999].

Table 1. Technical specifications for the RDC liquid-liquid extraction column.

RDC column geometry data in meter
Column height = 2.55
Rotor diameter = 0.09
Stator diameter = 0.105
Column diameter = 0.15
Compartment height = 0.03
Dispersed phase inlet = 0.25
Continuous phase inlet = 2.25

Table 2. Initial and inlet boundary conditions for the RDC liquid-liquid extraction column. $\mathcal{Z}$ represents the fluid flow domain, $B\mathcal{Z}_{\text{inlet}}$ the boundary of $\mathcal{Z}$ and $\delta(z-z_j)$ is the Dirac delta function. A_c, v^{in} (in stands for inlet), c_j^{in} and Q_j^{in} are defined as the column cross-sectional area, the feed mean droplet volume, the volumetric flow rate, and the inlet solute concentrations, respectively.

Initial conditions ($z \in \mathcal{Z}$, $t_0 = 0$)	Inlet boundary conditions ($t \in [t_0, \infty[$, $z \in B\mathcal{Z}_{\text{inlet}}$)
$N(z, t_0) = 0$	$N(z,t) = \delta(z - z_y) Q_y^{\text{in}} / v^{\text{in}} A_c$
$\alpha_y(z, t_0) = 0$	$\alpha_y(z,t) = \delta(z - z_y) Q_y^{\text{in}} / A_c$
$u_y(z, t_0) = 0$	$u_y(z,t) = \delta(z - z_y) (Q_y^{\text{in}} / A_c)^2$
$c_y(z, t_0) = 0$	$c_y(z,t) = \delta(z - z_y) Q_y^{\text{in}} c_y^{\text{in}} / A_c$
$c_x(z, t_0) = 0$	$c_x(z,t) = \delta(z - z_x) Q_x^{\text{in}} c_x^{\text{in}} / A_c$

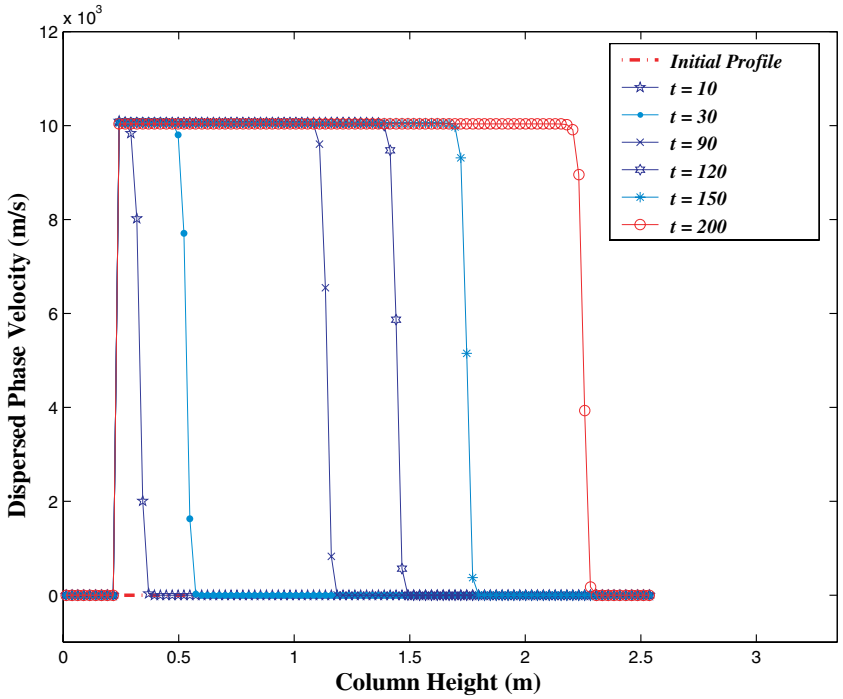

Fig. 1. Time history for the dispersed-phase velocity in the model system using the MUSCL–Hancock scheme based on splitting procedure together with SUPERBEE limiter on a mesh of 100 cells.

The initial and boundary conditions (inlet) that are used for the numerical solution are given in Table 2. These initial conditions constitute a difficult test, since they imply a strong discontinuity in all the flow variables. The computation has been carried out using the following constants for the Sauter mean droplet diameter d_{vs}, (8), and in the source term S_2, (10), are: $d_{\min} = 0.01\,\text{mm}$, $d_{\max} = 4.0\,\text{mm}$, $\rho_x = 1000.0\,\text{kg/m}^3$, $\rho_y = 860.0\,\text{kg/m}^3$, $\mu_x = 9.2 \times 10^{-4}\,\text{kg/ms}$, and $g = 9.81\,\text{m/s}^2$. The constants for the inlet boundary conditions in Table 2 are: $Q_y^{\text{in}} = 100.0\,\text{liter/h}$, $Q_x^{\text{in}} = 500.0\,\text{liter/h}$, $c_y^{\text{in}} = 0.0\,\text{kg/m}^3$, $c_x^{\text{in}} = 500.0\,\text{kg/m}^3$, v^{in} calculated using Eq. (8) with the inlet feed distribution $\bar{d}^{\text{in}} = 3.0\,\text{mm}$.

We have chosen to use the TVD MUSCL–Hancock scheme as a reference solution with a very fine mesh of 1000 cells within the splitting procedure. This scheme is then compared with the first-order upwind Godunov scheme, the Lax–Wendroff scheme, and the TVD MUSCL–Hancock scheme on a coarse mesh.

Figure 1 shows the time–evolution of the dispersed-phase velocity wave propagation profile for different time values ($t = 10, 30, 90, 120, 150,$ and 200). The results show that the multiple contact waves develop as time increases after the wave passes the inlet inside the column. Furthermore, one can see that the CFD-PBM coupled model develops a sharp shock wavefront at the boundary $z = z_y$ after a certain time

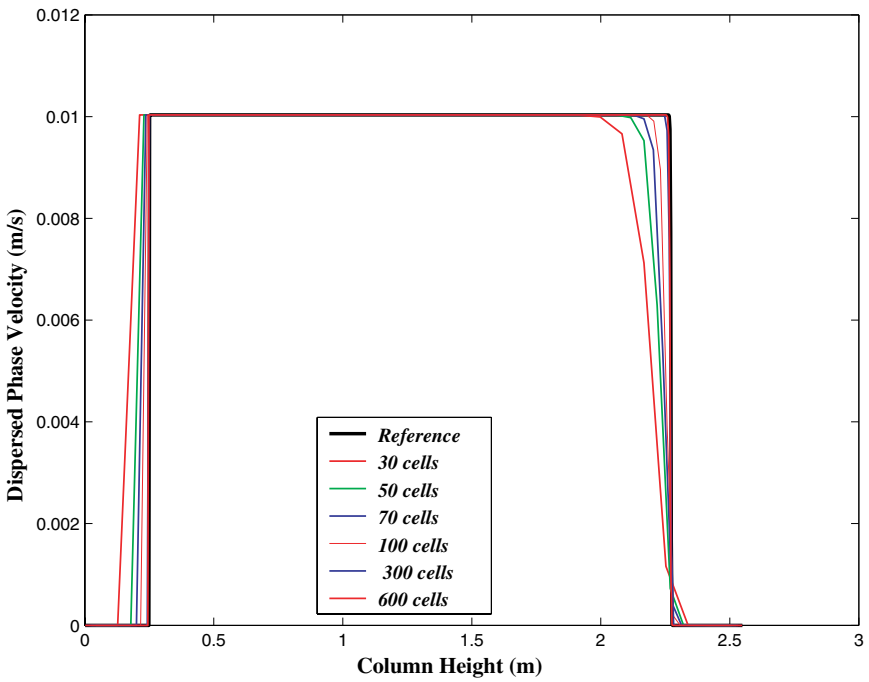

Fig. 2. Mesh refinement for the model system. Reference solution (thick line) and numerical solution (thin line) obtained by the TVD MUSCL–Hancock scheme based on splitting procedure at time $t = 200$.

of the propagation. Figure 1 results achieved using the MUSCL–Hancock scheme together with SUPERBEE limiter. This figure clearly shows that option $t = 200$ gives fairly good description for the two-phase flow inside the column and an excellent numerical results.

In order to test the convergence and stability of the TVD MUSCL–Hancock scheme a mesh convergence study displayed in Fig. 2 at $t = 200$ for a series of meshes from 30 to 1000 cells. There are no oscillations at the discontinuity when the mesh is refined. In this figure, it can be observed that the results are satisfactory and approaches the reference solution through which the dispersed phase move along the column. Further, from the figure, it can be seen that the mesh of 1000 cells is the best choice as a reference solution for this problem.

Figure 3 displays the dispersed-phase velocity profile at $t = 200$ for liquid-liquid two-phase flow with a mesh of 100 cells. The different methods are plotted for the sake of comparison, as shown in Fig. 3. It can be observed that the first-order Godunov scheme produces practically identical results, whereas the results with the Lax–Wendroff scheme are less accurate. However, the results of the TVD MUSCL–Hancock scheme smear the contact discontinuities better than the Lax–Wendroff

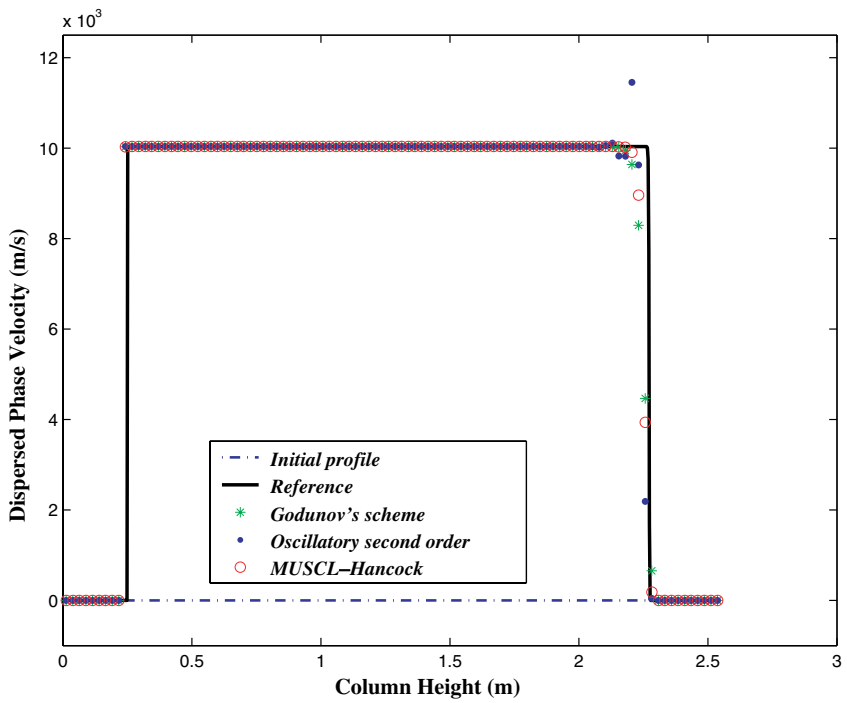

Fig. 3. Numerical solutions (symbols) for the model system using three numerical methods (TVD MUSCL–Hancock, Godunov, and Lax–Wendroff) are compared with the reference solution (thick line) at time $t = 200$ on mesh of 100 cells. The three methods are based on splitting procedure.

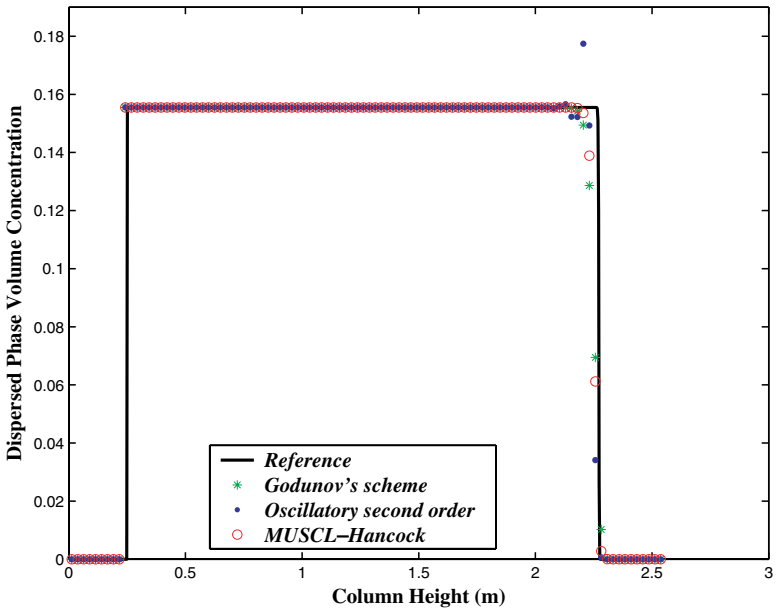

(a)

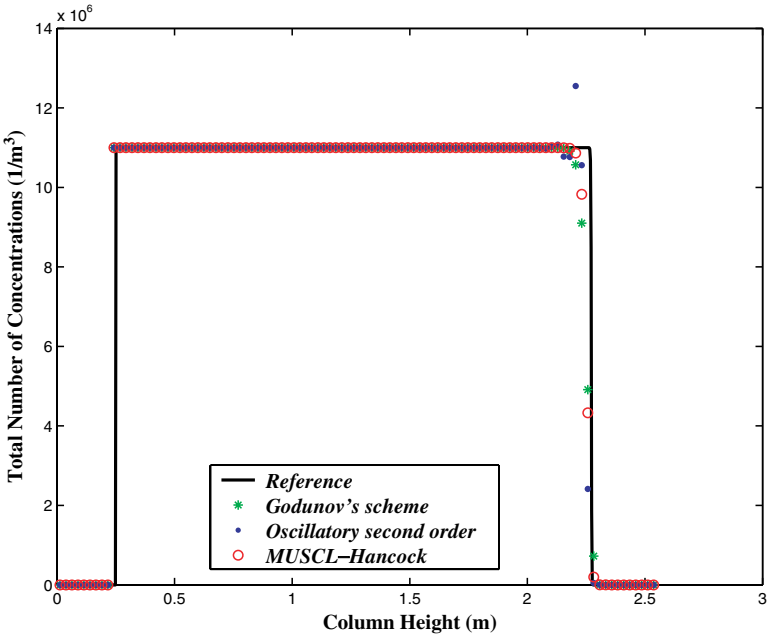

(b)

Fig. 4. Numerical solutions (symbols) for the model system at time $t = 200$ on mesh of 100 cells using the initial conditions given in Table 2. The solid black lines indicate the reference solution. (a) dispersed-phase volume concentration; (b) total number of concentrations; (c) continuous-phase velocity; (d) continuous-phase volume concentration.

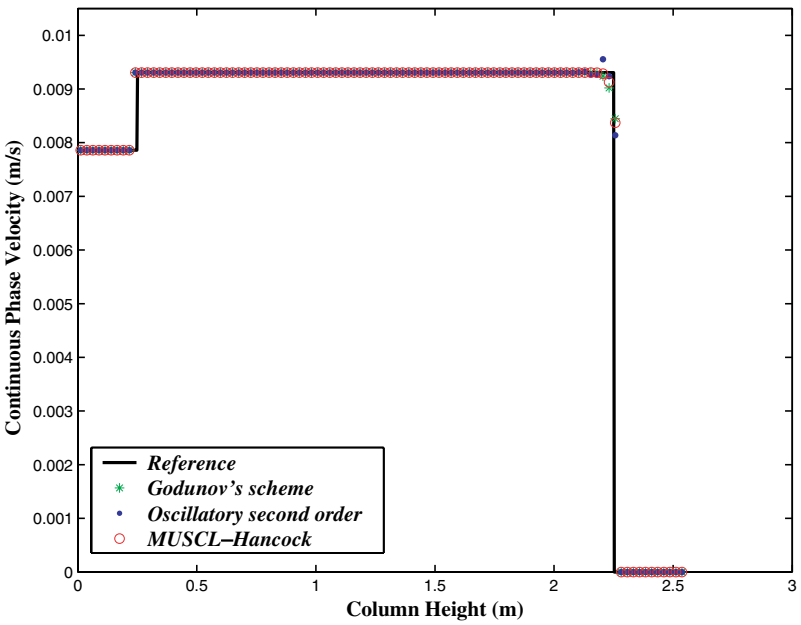

(c)

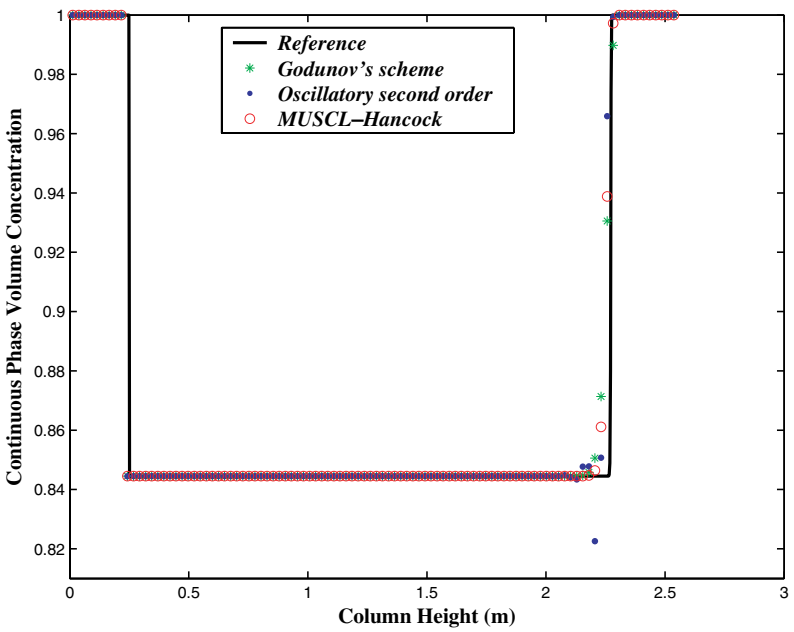

(d)

Fig. 4. (*Continued*)

and Godunov methods. This is clearly seen by the overshoot behavior of the numerical solution obtained by the Lax–Wendroff scheme in the vicinity of the contact waves.

The plots shown in Fig. 4 contain the numerical solutions for the dispersed-phase volume concentration, the total number of concentrations, and the velocity and volume concentration of the continuous phase at $t = 200$ on a mesh of 100 cells. Qualitatively, the three solutions are very similar, but the TVD MUSCL–Hancock scheme produces accurate results over the whole domain and capturing the sharp shocks very well indeed. Clearly, the solutions include a very sharp and moving wavefront and none of the Godunov and Lax–Wendroff methods computes the accurate position of this wavefront. Because of this sharp front, the Lax–Wendroff scheme suffers from numerical overshoot in the approximation of all flow variables.

To the authors opinion, the numerical splitting technique and the MUSCL–Hancock scheme together with the SUPERBEE limiter outperforms this test problem in an idealized manner and one could speculate that these numerical results are the most trustworthy. Unfortunately, we have no way of proving such a claim without experimental data. In the meantime, these implications to practical decision are significant and state that they should be widely applied in liquid-liquid extraction columns, and to develop the corresponding advanced numerical test problems. The results indicate that the upwind methods of Godunov type based on Strang splitting approach give more accurate solutions than the traditional centered numerical methods, even for fairly coarse mesh. They fail to resolve this sharp front wave associated with the CFD-PBM coupled model proposed in this paper and further research is needed in this direction.

6. Conclusions

In this present work, we have proposed and developed a comprehensive mathematical framework and Godunov methods of upwind–type based on splitting procedure for a CFD-PBM coupled model that can be used for the numerical simulation of 1D liquid-liquid two-phase flow in an extraction column. The PBM based on the concept of primary and secondary particle approaches is coupled with the momentum equation for the dispersed phase. A characteristic analysis informs that the model equations are hyperbolic with real eigenvalues. These eigenvalues are equal to the dispersed and continuous phases. Through a detailed analysis, the derived eigenvectors corresponding to these eigenvalues are shown to be linearly degenerated. Furthermore, the nature of characteristic fields confirms that the developed CFD-PBM coupled model will have contact discontinuities only as a wave solution.

Having established this mathematical foundation for the CFD-PBM coupled model, numerical approximations were constructed for the model. These numerical solutions are based on a fairly general splitting approach. This allows the use of Godunov methods of upwind type for the numerical solution of the homogeneous problem and for the special treatment for the source terms appearing in the model.

The splitting technique and Godunov methods of upwind type represent a competitive alternative to the existing numerical methods for simulating of liquid-liquid extraction columns. These methods have been applied to the calculation of a two-phase flow problem within a liquid-liquid extraction column. Numerical results show that the considered numerical methods are robust with the ability to capture solutions accurately. In particular, it has been demonstrated that the MUSCL–Hancock scheme with SUPERBEE limiter gives a very sharp and accurate resolution, and able to produce smeared results in regions near discontinuities.

A large amount of work is required in order to understand better the challenging environments found in liquid-liquid extraction columns. It is, therefore, believed that liquid-liquid extraction columns have a need of well-defined physical mathematical models in combination with appropriate numerical methods. To the best of our knowledge, this is the first time that a CFD-PBM coupled model for liquid-liquid extraction columns is calculated by Godunov methods of upwind type. The mathematical and numerical studies presented in this paper reveal an improved performance and provide a useful foundation for further studies of the full model upon inclusion of exchange source terms such as the droplet breakage and coalescence and the mass transfer coefficients. In addition, the numerical methods can be extended to handle the CFD-PBM coupled in more space dimensions. These paths are under consideration for future research.

Acknowledgments

This work has been supported by the German Research Association (DFG) through the grant (DFG Ba 1569/36–1 and DFG Ku 1430/4–1) under the title "Coupling of Population Balance Equations with Computational Fluid Dynamics (CFD)". The support from the Higher Council for Science and Technology (HCST) in Jordan is greatly acknowledged. The authors are very grateful to these funding agencies for this support.

References

Attarakih, M., Bart, H.-J. and Faqir, N. [2006] Numerical solution of the bivariate population balance equation for the interacting hydrodynamics and mass transfer in liquid–liquid extraction columns, *Chem. Eng. Sci.* **6**, 113–123.

Attarakih, M. *et al.* [2008] Dynamic modelling of liquid extraction columns using the direct primary and secondary particle method (DPSPM). In Proceedings of the 6th International Conference on CFD in Oil & Gas, Metallurgical and Process Industries. SINTEF/NTNU, Trondheim, Norway.

Chadwick, P. [1976] *Continuum Mechanics: Concise Theory and Problems*, Wiley.

Fraccarollo, L. and Toro, E. F. [1995] Experimental and numerical assessment of the shallow water model for two-dimensional dam-break type problems, *J. Hydraulic Res.* **33**, 843–864.

Gelbard, F., Tambour, Y. and Seinfeld, J. H. [1980] Sectional representations for simulating aerosol dynamics, *J. Colloid Interface Sci.* **76**, 541–556.

Godunov, S. K. [1959] Finite difference methods for the computation of discontinuous solutions of the equations of fluid dynamics, *Matematicheskii Sbornik* **47**, 271–306.

Colella, D. *et al.* [1999] A study on coalescence and breakage mechanisms in three different bubble columns, *Chem. Eng. Sci.* **54**, 4767–4777.

Gourdon, C., Casamatta, G. A. and Muratet, G. [1994] Population balance based modelling, in (Eds.), Godfrey, J. C. and Slater, M. J. John Wiley & Sons, *Liquid–Liquid Extraction Equipment*, pp. 141–226.

Gunawan, R., Fusman, I. and Braatz, R. D. [2004] High resolution algorithms for multidimensional population balance equations, *AIChE J.* **50**, 2738–2749.

Hounslow, M. J., Ryall, R. L. and Marshall, V. R. [1988] A discretized population balance for nucleation, growth and aggregation, *AIChE J.* **34**, 1821–1832.

Hufnagl, H., McIntyre, M. and Bla$B$, E. [1991] Dynamic behaviour and simulation of a liquid–liquid extraction column, *Chem. Eng. Technol.* **14**, 301–306.

Hulburt, H. M. and Katz, S. [1964] Some problems in particle technology: A statistical mechanical formulation, *Chem. Eng. Sci.* **19**, 555–574.

Kostoglou, M. and Karabelas, A. J. [1994] Evaluation of zero order methods for simulating particle coagulation, *J. Colloid Interface Sci.* **163**, 420–431.

Kronberger, T. *et al.* [1995] Numerical simulation of extraction columns using a drop population model, *Comput. Chem. Eng.* **19**, S639–S644.

Laney, C. B. [1998] *Computational Gasdynamics*, Cambridge University Press.

Lee, M. H. [2001] A survey of numerical solutions to the coagulation equation, *J. Phys. A Math. Theor.* **34**, 10219–10241.

Ma, D. L., Tafti, D. K. and Braatz, R. D. [2002] High resolution simulation of multidimensional crystal growth, *Indus. Eng. Chem. Res.* **41**, 6217–6223.

Maisels, A., Kruis, F. E. and Fissan, H. [1999] Direct Monte Carlo simulations of coagulation and aggregation, *J. Aerosol Sci.* **30**, 417–418.

Marchal, P. *et al.* [1988] Crystallization and precipitation engineering — I. An efficient method for solving population balance in crystallization with agglomeration, *Chem. Eng. Sci.* **43**, 59–67.

Muhr, H. *et al.* [1996] Crystallization and precipitation engineering — VI. Solving population balance in the case of the precipitation of silver bromide crystals with high primary nucleation rates by using the first order upwind differentiation, *Chem. Eng. Sci.* **51**, 309–319.

Ramkrishna, D. [2000] *Population Balances: Theory and Applications to Particulate Systems in Engineering*, Academic Press.

Rhee, R., Aris, R. and Amundson, N. R. [2001] *First–Order Partial Differential Equations, Volume 1: Theory and Applications of Single Equations*, Dover Publications.

Romenski, E. and Toro, E. F. [2004] Compressible two-phase flow models: two-pressure models and numerical methods, *Comput. Fluid Dyn. J.* **13**, 403–416.

Schiller, L. and Naumann, A. [1933] Über die grundlegenden Berechnungen bei der Schwerkraftaufbereitung, *Ver. Deut. Ing.* **77**, 318–320.

Schmidt, S. A. *et al.* [2006] Droplet population balance modelling — hydrodynamics and mass transfer, *Chem. Eng. Sci.* **61**, 246–256.

Shah, B. H., Ramkrishna, D. and Borwanker, J. D. [1977] Simulation of particulate systems using the concept of the interval of quiescence, *AIChE J.* **23**, 897–904.

Singh, P. N. and Ramkrishna, D. [1977] Solution of population balance equations by MWR, *Comput. Chem. Eng.* **1**, 23–31.

Strang, G. [1968] On the construction and comparison of difference schemes, *SIAM J. Numer. Anal.* **5**, 506–517.

Sychev, V. V. *et al.* [2008] *Asymptotic Theory of Separated Flows*, Cambridge University Press.

Tiwari, S. and Kuhnert, J. [2007] Modeling of two-phase flows with surface tension by Finite Pointset Method (FPM), *J. Comp. Appl. Math.* **203**, 376–386.

Toro, E. F. [1999] *Riemann Solvers and Numerical Methods for Fluid Dynamics*, Springer Verlag.

van Leer, B. [1979] Towards the ultimate conservative difference scheme, V: A second order sequel to Godunov's method. *J. Comput. Phys.* **32**, 101–136.

Vanni, M. [2000] Approximate population balance equations for aggregation–breakage processes, *J. Colloid Interface Sci.* **221**, 143–160.

Vikhansky, A. and Kraft, M. [2004] Modelling of a RDC using a combined CFD–population balance approach, *Chem. Eng. Sci.* **59**, 2597–2606.

Weinstein, O., Semiat, R. and Lewin, D. R. [1998] Modeling, simulation and control of liquid–liquid extraction columns, *Chem. Eng. Sci.* **53**, 325–339.

Xiaojin, T., Guangsheng, L. and Jiading, W. [2005] An improved dynamic combined model for evaluating the mass transfer performances in extraction columns, *Chem. Eng. Sci.* **60**, 4409–4421.

Yanenko, N. N. [1971] *The Method of Fractional Steps*, Springer-Verlag.

Zeidan, D. *et al.* [2007a] Numerical study of wave propagation in compressible two-phase flow, *Int. J. Numer. Methods Fluids* **54**, 393–417.

Zeidan, D. *et al.* [2007b] Numerical solution for hyperbolic conservative two-phase flow equations, *Int. J. Comput. Methods* **4**, 299–333.

Zucca, A. *et al.* [2006] Implementation of population balance equation in CFD codes for modelling soot formation in turbulent flames, *Chem. Eng. Sci.* **61**, 87–95.